J Mater Sci (2008) 43:5644–5646
DOI 10.1007/s10853-008-2881-x

LETTER

Deformation behavior and mechanism of porous PLLA under compression

Mitsugu Todo · Hiroyuki Kuraoka · Jinwoong Kim · Kentaro Taki · Masahiro Ohshima

Received: 1 July 2008 / Accepted: 15 July 2008 / Published online: 25 July 2008

Bioabsorbable polymers such as poly(L-lactide) (PLLA) and poly(L-lactide-co-DL-lactide) (PLDL) have been considered to be used as scaffolds in tissue engineering [1–3]. Recently, composite scaffolds of such polymers and bioactive inorganic materials such as hydroxyapatite have also been investigated to improve bioactivity of the polymeric scaffolds [4–9]. These scaffolds usually have porous structures to culture and multiply cells inside the pores, and these pores should be connected with each other to ensure cell growth. These scaffolds are planned to be implanted into injured target tissues for regeneration, and hence, the scaffolds need to have proper mechanical properties to be mechanically compatible with the surrounding tissues. It is therefore important to develop scaffolds with desired mechanical properties by controlling their structures and constituents. However, most of the previous studies focused on processing techniques and biocompatibility of scaffolds, and few attempts have been made to investigate the relationship between mechanical behavior and the structure.

In the present study, PLLA continuous-porous structures were developed from pelletized PLLA by using the solid–liquid phase separation and the freeze-drying methods [4]. First, PLLA pellets were dissolved in 1,4-dioxane to make 3, 5, and 7 wt.% solutions. The solid–liquid phase separation technique and a subsequent solvent sublimation process were used to generate the highly porous PLLA scaffolds. The PLLA dioxane solutions in test tubes were cooled from the bottom surfaces at a constant rate by using liquid nitrogen to induce solid–liquid phase separation. The phase-separated samples were then dried under vacuum at −5 °C for about 6 days to remove the solvent completely. Cylindrical samples were obtained and then trimmed to be a cylinder with 8-mm diameter and 12-mm length. Porosity (volume fraction of pores) of a scaffold was estimated from the densities of PLLA solid and the scaffold. Compression tests were then performed using a conventional mechanical testing machine at a loading rate of 1 mm/min. A field-emission scanning electron microscope (FE-SEM) was also used to observe the microstructures of the porous samples and the deformation behavior of the porous samples at the critical point.

FE-SEM micrographs of the cross-sections in the transverse direction are shown in Fig. 1. Homogeneous distribution of pores is observed, and the size of the pores tends to decrease with increase in the concentration of the solution. The porosities of these porous samples were estimated as 94.7, 90.0, and 88.5% for the concentrations of 3, 5, and 7 wt.%, respectively. FE-SEM micrograph of a cross-section in the vertical direction is shown in Fig. 2. For all the samples, this kind of porous structure was observed. These structures shown in Figs. 1 and 2 suggest that the crystals of the solvent grow in the vertical and transverse directions at a constant speed by the freezing process. Typical stress–strain curves under compression are shown in Fig. 3. The stress–strain relation of this porous structure of PLLA can be characterized by four different regions as shown in Fig. 4. The region A is the initial linear portion corresponding to linear elastic deformation of the porous structure. The end of the region A and the transition point to the region B is recognized as a critical point where localized failures of the wall structures of the pores take place. In the region B, stress

M. Todo (✉) · H. Kuraoka
Research Institute for Applied Mechanics, Kyushu University, 6-1 Kauga-koen, Kasuga, Fukuoka 816-8580, Japan
e-mail: todo@riam.kyushu-u.ac.jp

J. Kim · K. Taki · M. Ohshima
Department of Chemical Engineering, Kyoto University, Katsura Campus, Kyoto 615-8510, Japan

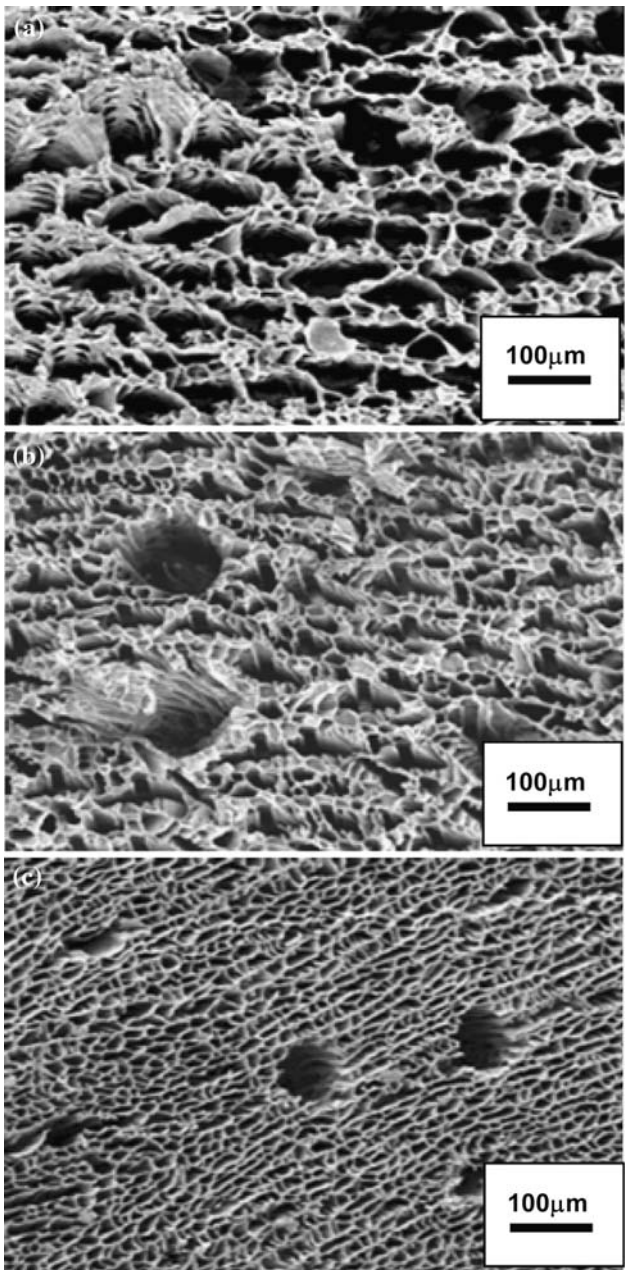

Fig. 1 FE-SEM micrographs of cross-sections in the transverse directions. (**a**) 3 wt.% (**b**) 5 wt.%, and (**c**) 7 wt.%

becomes almost constant during such failure process, and stress starts to increase again when the failure process reaches its saturation corresponding to gradual disappearance of the pores, denoted as the region C. The region D is the second linear portion corresponding to the linear elastic behavior of the bulk structure with totally disappeared pores. FE-SEM micrograph of the failure behavior at the critical point, the transition point from A to B, is shown in Fig. 5. It is clearly seen that localized buckling occurs under compression. Dependence of the porosity on the compressive strength and elastic modulus is shown in Fig. 6.

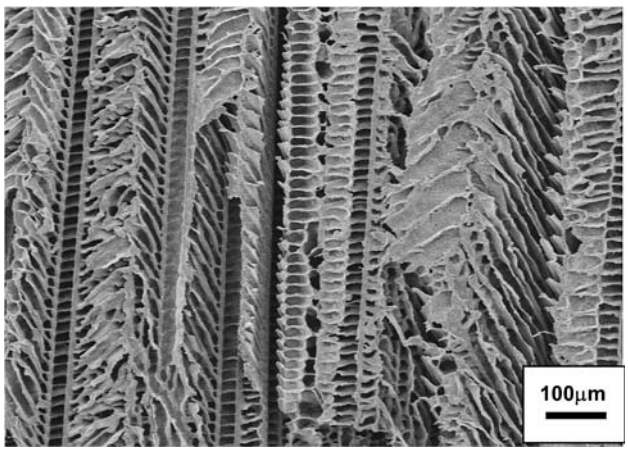

Fig. 2 FE-SEM micrograph of longitudinal section (7 wt.%)

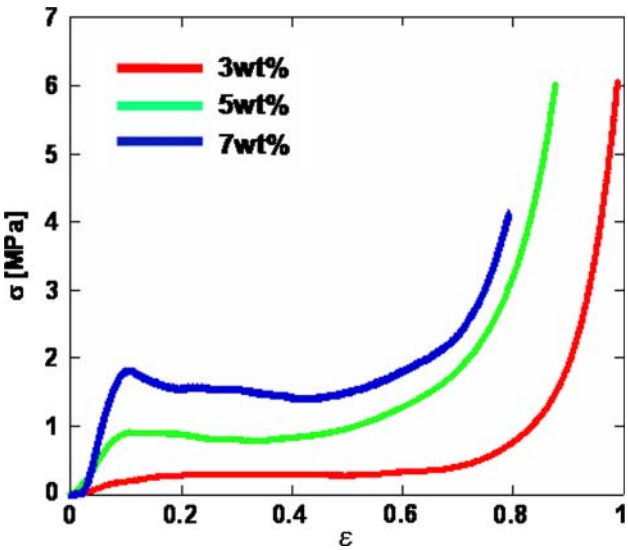

Fig. 3 Stress–strain curves under compression

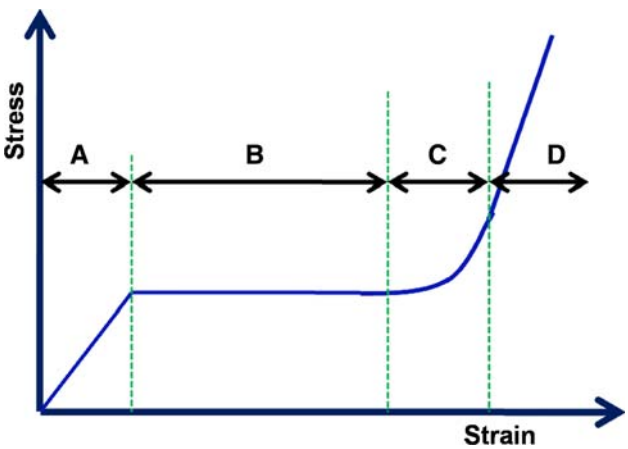

Fig. 4 Four different regions appearing in stress–strain relation

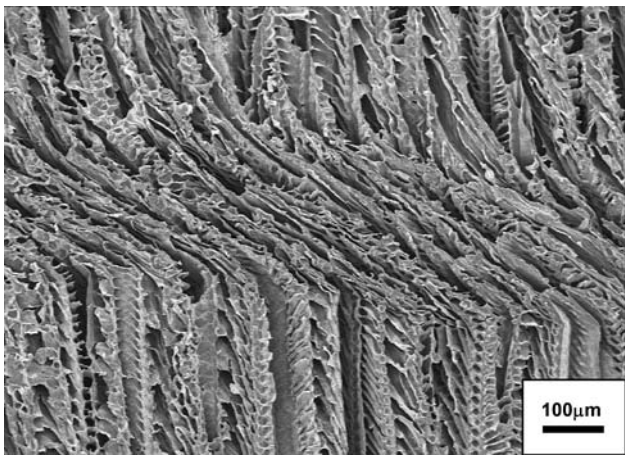

Fig. 5 Deformed specimen at critical stress (7 wt.%)

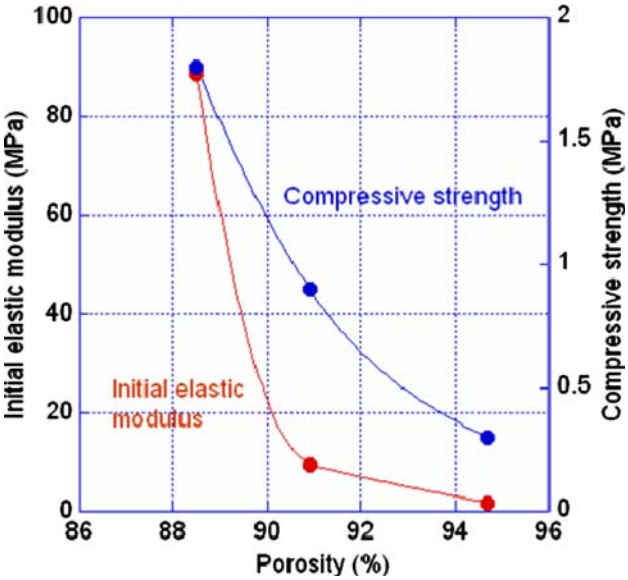

Fig. 6 Dependence of initial elastic modulus and compressive strength on porosity

The compressive strength is defined as the stress at the critical point, where localized bucking starts to form. It is seen that both the strength and modulus decrease rapidly with increase in porosity.

In summary, porous structures of PLLA were successfully developed by using the solid–liquid phase separation technique and the subsequent solvent sublimation process. It was found that the porosity and the size of pores can be controlled by changing the mixing ratio of PLLA and dioxane. Furthermore, homogeneous porous structures can be obtained by freezing the solution at a constant speed. It is also noted that the end of linear elastic deformation is characterized by the initiation of localized bucking behavior.

References

1. Mikos AG, Thorsen AJ, Czerwonka LA, Bao Y, Langer R (1993) Polymer (Guildf) 35:1068. doi:10.1016/0032-3861(94)90953-9
2. Howard D, Partridge K, Yang X, Clarke NMP, Okubo Y, Bessho K et al (2002) Biochem Biophys Res Commun 299:208. doi:10.1016/S0006-291X(02)02561-5
3. Lin ASP, Barrows TH, Cartmell SH, Guldberg RE (2003) Biomaterials 24:481. doi:10.1016/S0142-9612(02)00361-7
4. Zhang R, Ma PX (1999) J Biomed Mater Res 44:446. doi:10.1002/(SICI)1097-4636(19990315)44:4<446::AID-JBM11>3.0.CO;2-F
5. Ma PX, Zhang R, Xiao G, Franceschi (2001) J Biomed Mater Res 54:284. doi:10.1002/1097-4636(200102)54:2<284::AID-JBM16>3.0.CO;2-W
6. Wei G, Ma PX (2004) Biomaterials 25:4749. doi:10.1016/j.biomaterials.2003.12.005
7. Teng X, Ren J, Gu S (2007) J Biomed Mater Res Part B 81B:185. doi:10.1002/jbm.b.30652
8. Georgiou G, Mathieu L, Pioletti DP, Bourban PE, Manson JAE, Knowles JC et al (2007) J Biomed Mater Res Part B 80B:322. doi:10.1002/jbm.b.30600
9. Woo KM, Seo J, Zhang R, Ma PX (2007) Biomaterials 28:2622. doi:10.1016/j.biomaterials.2007.02.004